AFRL-SN-RS-TR-2005-154
Final Technical Report
April 2005

OPTICALLY ASSISTED HIGH-SPEED, HIGH RESOLUTION ANALOG-TO-DIGITAL CONVERSION

University of Florida

APPROVED FOR PUBLIC RELEASE; DISTRIBUTION UNLIMITED.

AIR FORCE RESEARCH LABORATORY
SENSORS DIRECTORATE
ROME RESEARCH SITE
ROME, NEW YORK

STINFO FINAL REPORT

This report has been reviewed by the Air Force Research Laboratory, Information Directorate, Public Affairs Office (IFOIPA) and is releasable to the National Technical Information Service (NTIS). At NTIS it will be releasable to the general public, including foreign nations.

AFRL-SN-RS-TR-2005-150 has been reviewed and is approved for publication

APPROVED: /s/
JAMES R. HUNTER
Project Engineer

FOR THE DIRECTOR: /s/
RICHARD G. SHAUGHNESSY
Chief, Rome Operations Office
Sensors Directorate

REPORT DOCUMENTATION PAGE

Form Approved
OMB No. 074-0188

1. AGENCY USE ONLY (Leave blank)	2. REPORT DATE	3. REPORT TYPE AND DATES COVERED
	April 2005	**Final** **Aug 03 – Aug 04**

4. TITLE AND SUBTITLE

OPTICALLY ASSISTED HIGH-SPEED, HIGH RESOLUTION ANALOG-TO-DIGITAL CONVERSION

5. FUNDING NUMBERS

G - F30602-03-2-0219
PE - 62500F
PR - 528D
TA - SN
WU - 01

6. AUTHOR(S)

Henry Zmuda

7. PERFORMING ORGANIZATION NAME(S) AND ADDRESS(ES)

University of Florida
Graduate Engineering and Research Center
1350 North Poquito Road
Shalimar FL 32579

8. PERFORMING ORGANIZATION REPORT NUMBER

N/A

9. SPONSORING / MONITORING AGENCY NAME(S) AND ADDRESS(ES)

AFRL/SNDP
26 Electronic Parkway
Rome NY 13441-4514

10. SPONSORING / MONITORING AGENCY REPORT NUMBER

AFRL-SN-RS-TR-2005-154

11. SUPPLEMENTARY NOTES

AFRL Project Engineer: James R. Hunter/SNDP/(315) 330-7045 James.Hunter@rl.af.mil

12a. DISTRIBUTION / AVAILABILITY STATEMENT

APPROVED FOR PUBLIC RELEASE; DISTRIBUTION UNLIMITED.

12b. DISTRIBUTION CODE

13. ABSTRACT ***(Maximum 200 Words)***

An approach that modifies an analog fiber optic link with a recirculating optical loop as a means to realize a high-speed, high-resolution Analog-to-Digital Converter (ADC) is presented. The loop stores a time-limited microwave signal so that it may be digitized by using a slower, conventional electronic ADC. Detailed analytical analysis of the dynamic range and noise figure shows that under appropriate conditions the microwave signal degradation is sufficiently small so as to allow the digitization of a multi-gigahertz signal with a resolution greater than 10 effective bits. Experimental data is presented which shows that a periodic extension of the input signal can be sustained for well over one hundred periods that in turn suggests an electronic ADC speed-up factor of over 100. The data also shows that polarization effects must be carefully managed to inhibit the loops tendency to lase even though the loop itself contains no frequency-selective elements.

14. SUBJECT TERMS

Optical analog-to-digital converter (ADC), Photonic ADC, ultra fast ADC, photonically assisted ADC, photonic digitizer

15. NUMBER OF PAGES 27

16. PRICE CODE

17. SECURITY CLASSIFICATION OF REPORT	18. SECURITY CLASSIFICATION OF THIS PAGE	19. SECURITY CLASSIFICATION OF ABSTRACT	20. LIMITATION OF ABSTRACT
UNCLASSIFIED	UNCLASSIFIED	UNCLASSIFIED	UL

TABLE OF CONTENTS

LIST OF FIGURES

Page

LIST OF TABLES

Page

1. INTRODUCTION

The analog-to-digital converter (ADC) is essential for the collection of analog sensor data and converting it to a binary representation suitable for digital processing. Electronic warfare, communications, digital radio, and electronic instrumentation are but a few of the applications where a high-speed, high-resolution ADC would greatly enhance the system performance. The realization of such an ADC has proven itself a difficult task, and the potential for using optical processing as a means to achieve high-speed conversion has long intrigued system designers [1,2]. Although there has been significant progress with high-speed electronic ADC systems, the ability to achieve conversion rates (at least 10^{10}-samples per second) at a reasonable resolution (greater than 4 - 6 bits) remains an elusive goal [3, 4].

Though a wide variety of approaches exist for the implementation of an all-photonic high speed ADC [5-10], much emphasis has been placed on taking full advantage of advances in electronic ADC technology [11-14]. The latter type of approach is generally termed an *optically assisted* ADC, and uses optical techniques to condition the high-speed signal to be digitized in such a way that a comparatively lower-speed electronic ADC can be used to perform the actual digitization. Such an approach is especially attractive in that it allows the optical ADC architecture to keep pace with advances in electronic ADC technology. Specifically, as the speed and resolution of electronic ADC's continue to improve, the optical portion of the system is used to further enhance the performance of the overall system.

This report shows how a conventional analog fiber optic link can be augmented with a recirculating optical delay loop so as to realize an optically assisted ADC that provides improved performance in terms of both speed and resolution using one (comparatively slow) electronic ADC. The overall architecture is quite simple and readily integrates with any electronic ADC system. Moreover, the high-speed ADC performance is fundamentally limited by the performance of the fiber optic link. Since high fidelity fiber optic links, specifically links having a large dynamic range, are the subject of ongoing research, improved link performance will translate directly to improved ADC performance. The approach also has the distinct advantage

in that it can be configured to provide both high-speed and high resolution thereby avoiding the speed-resolution tradeoffs that have plagued ADC system designers.

Section 2 of this report explains the overall system operation, specifically the speed-resolution tradeoff, by quantifying how the recirculating delay loop degrades the fiber optic link performance, and finally Section 3 presents proof-of-principle experimental results. These experimental results show that a replica of the input microwave signal is present for over 100 periods suggesting a speed-up factor for an electronic ADC of the same amount. The system was constructed using components that were all polarization insensitive. This resulted in most instances in a return optical signal that was like-polarized with the input optical signal. Since the gain of the recirculating loop is adjusted to unity, there was a tendency for the system to lase. Since the loop contained no wavelength selective components, lasing could not occur in the strict sense. However, naturally occurring peaks in the optical amplifiers spectral response resulted in random temporal "bursts" of optical signal appearing as added noise in the detected RF signal. To eliminate this from occurring, a means of managing the loop polarization is shown later in the report, but experimental results have not been obtained for this modification to date.

2. SYSTEM OPERATION

2.1 Timing and Bandwidth Considerations

For the purposes of the present discussion it is assumed that sampling rates are determined from the Nyquist criteria, namely that an RF signal whose highest frequency component is $f_{\max}$ requires a sampling rate of s_f samples per second, corresponding to a sampling interval of T_f, where $T_f = s_f^{-1} = \left(2 f_{\max}\right)^{-1}$. Figure (1-a) shows that a signal of duration of T seconds would require $N = \text{integer}\left(T \cdot s_f\right)$ high-speed samples, while Figure (1-b) shows how these same N sample values can be (ideally) captured from the periodic extension of the time-limited RF input. This in turn allows the input signal to be digitized using a (comparatively slow) ADC, sampling at a reduced rate with associated sampling interval T_s, where $T_s = T + T_f$. Thus, successive *samples* of the high-speed signal can be acquired from properly timed successive *periods* of the input signal. It is seen then that the required N high-speed samples can be captured from N periods. The number of periods required to capture the necessary input

information thus represents a fundamental parameter in the analysis to follow. Note however that the timing jitter requirements (aperture uncertainty) are the same as those for the high-speed ADC, an issue examined later in this report. The time-limited requirement of the signal also provides a low frequency limit of $f_{\min} = 2T_s^{-1}$, though this is of lesser significance than maximum frequency, it does pose an engineering issue relating the maximum frequency, bandwidth, and number of samples that would need to be addressed for a given application.

2.2 Photonic System

A block diagram showing the details for modifying an analog fiber optic link with a recirculating (optical) delay line so as to produce the periodic extension of the microwave input signal as well as the associated low-speed ADC is shown in Figure (2). Referring to Figure (2), the signal to be digitized first amplitude modulates a CW laser. The signal conditioning shown provides for sign-bit extraction and any amplification, level shifting, or band limiting that may be required for optimal link performance. Such signal preconditioning is present in any ADC and is not considered further in this report. For proper operation of the system it is imperative that the RF input signal be strictly time-limited, and this can be accomplished in a number of ways. Figure (2) shows an optical switch (OS) at the output of the modulator. This switching operation can be realized in the optical domain, for example, with a high-speed electrooptic or acoustooptic switch or an electroabsorption modulator that interrupts the optical path after the required length of time. Alternatively, the time-limiting operation can be performed electronically at the input to the amplitude modulator. This optically modulated, time limited RF signal is then injected into the recirculating loop by means of an optical coupler. The purpose of the recirculating delay (with a loop transit time of T seconds) is to produce the (nominally) periodic replicas of the input signal of period T as discussed. The recirculating loop contains a semiconductor optical amplifier (SOA) to compensate for any losses in the loop and an isolator to insure one-way loop circulation. An appropriate length of optical fiber is used to (roughly) establish the necessary time delay T while a variable delay line trimmer is included to precisely adjust the loop delay to the exact value. This required loop length can be computed, assuming that the signal essentially propagates in optical fiber as $L = c\dfrac{T_s}{n_f}$ where c is the speed of light in free space and n_f is the fiber group index.

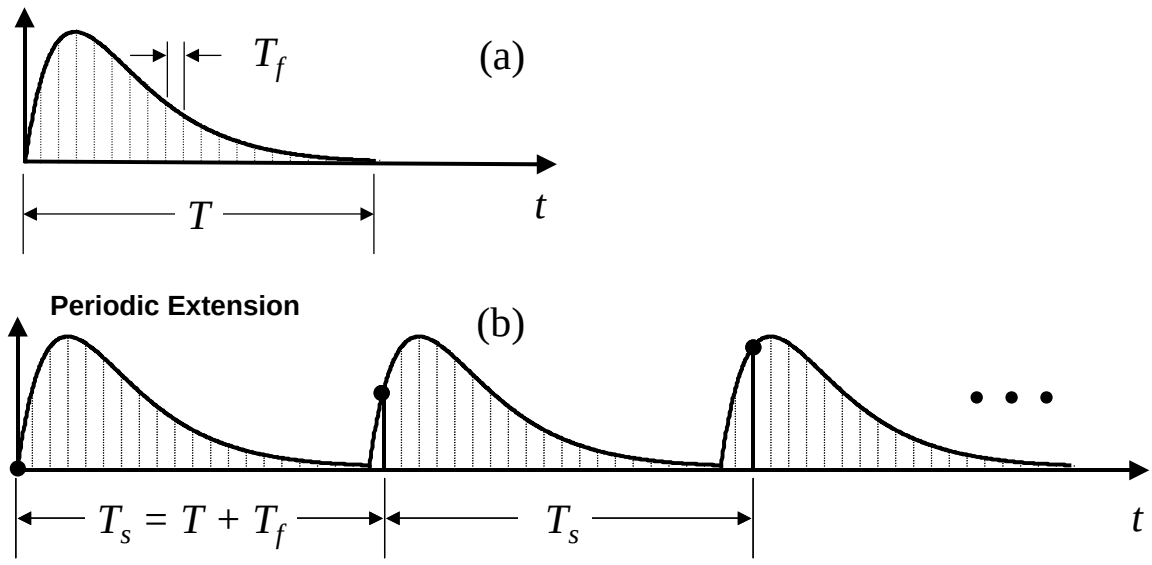

Figure 1: (a) Nyquist sampled signal and (b) equivalent, reduced-rate samples extracted from periodic replicas of the original signal.

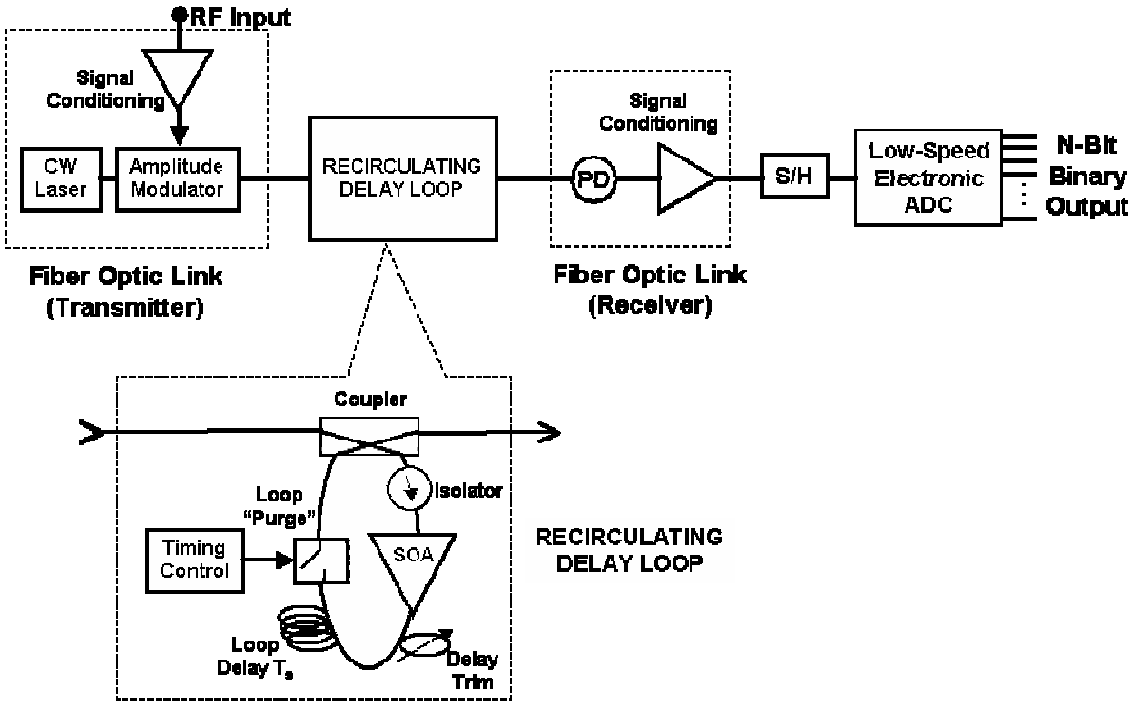

Figure 2: Block diagram of the modification of a fiber optic link with a recirculating delay line to realize an optically assisted ADC.

To prevent time-aliasing as the optically modulated RF signal recirculates, a second time limiting optical switch is also included in the delay loop as a means to purge the recirculating signal once the digitalization process is completed so that the operation may start again with the next input signal packet to be digitized. If the gain of the SOA were adjusted to exactly compensate for the loss, the system would essentially act as a ring cavity laser resonating at frequencies where the loop phase-shift is an integer multiple of 2π. Since the loop time delay is relatively long, perhaps as long as several microseconds, the loop will support a very large number of resonances. With the lack of any frequency selective device in the loop, lasing at any particular wavelength(s) is not likely. Under proper operating conditions, the coherent addition of the optically-modulated RF signal will never occur in the loop. This suggests that if necessary, a polarization scrambler can be included in the loop, resulting in a polarization dependent loss that is not compensated by the SOA gain and hence completely suppress any laser oscillations. Upon exiting the loop via the input/output coupler, the delayed, RF modulated optical signal is detected and demodulated by a high-speed photodetector. Note also that the first pulse to exit the system will not have traversed the recirculating delay loop but rather passes directly through the input/output coupler. Because of the possible disparity in amplitude level this pulse may not be directly usable as part of the signal to be digitized. It can however be useful as a header signal indicating to the electronic ADC system that an input signal is forthcoming. Once again, if necessary, the detected electrical signal may be appropriately conditioned before being digitized by the low-speed ADC.

As Figure (2) suggests, with the exception of the recirculating delay loop, the remaining components consist simply of a conventional fiber optic link. Clearly then the performance of the complete system will be ultimately limited by the performance of the fiber link used. The analysis to follow will thus concentrate on how the inclusion of the recirculating delay line degrades the performance of this fiber link. Once this degradation has been quantified, the link specification needed to meet an overall ADC performance requirement can be stated.

Proper evaluation of the performance of the ADC system requires that several factors be quantified. These include the exact nature of the loop timing, the degradation in the dynamic range of the RF input signal with each loop circulation, the restrictions on the input signal-to-noise ratio (SNR) so as to achieve a specified effective number of bits for the ADC, and timing jitter (aperture uncertainty), and these factors are now examined.

2.3 Noise Figure, Signal-to-Noise Ratio, and Effective Number of Bits

In addition to the ADC conversion speed, another major factor limiting the ADC performance is the effective number of bits (ENOB). This is generally expressed in terms of the dynamic range of the overall system. For a broadband fiber optic link, the dynamic range is limited by intermodulation products introduced by the modulator nonlinearities. The maximum allowable RF input signal that can be applied to the modulator occurs when the power contained in the first intermodulation product at the output just equals the power in the noise floor. This defines the spur-free dynamic range (SFDR) or the maximum SNR. The maximum allowable input voltage determines the full-scale voltage V_{FS}. For a B-bit ADC, the full-scale voltage is expressed as $V_{FS} = 2^B V_{LSB}$, where V_{LSB} is the minimum voltage (corresponding to the least significant bit) that can be resolved. For an arbitrary input signal, it is usual to assume that the signal quantization error is uniformly distributed over the sampling interval which results in an rms noise voltage of $V_{noise_{rms}} = \frac{V_{LSB}}{\sqrt{12}}$ [3]. The ratio of the rms value of the full-scale voltage to $V_{noise_{rms}}$ gives the classical result relating the SNR and resolution (ENOB) *B*, namely

$$SNR = \frac{3}{2} 2^{2B} \tag{1}$$

Equation (1) establishes the ENOB available from and ADC due to the SNR alone. The inclusion of the recirculating loop will degrade the dynamic range of the link. The degradation in the SNR of the RF-input signal as it propagates through the recirculating delay loop the required N number of times is readily characterized by the overall system noise figure, defined as

$$F_{RF}(N) = \left. \frac{SNR_{without\ recirculating\ loop}}{SNR_{with\ recirculating\ loop}} \right|_{Same\ Gain} \tag{2}$$

assuming the same RF link gain for both cases.

Referring again to Figure 2, let $L_I > 1$ denote the isolator loss, $L_c > 1$ the coupling ratio (splitting and excess loss), $L_t > 1$ is the corresponding coupler through insertion loss,

and $L_{ex} > 1$ the total excess loop loss arising from connector loss as well as any other losses present in the loop. Also denote the gain of the optical amplifier as G_{SOA} with corresponding noise figure F_{SOA}. A straightforward analysis shows that the loop noise figure is

$$F_{Loop} = L_I \left(F_{SOA} + \frac{L_{ex} L_t - 1}{G_{SOA}} \right) \tag{3}$$

As the RF modulated optical signal circulates around the loop, the signal-to-noise ratio degrades with each pass. For the $N^{\underline{\text{th}}}$ loop circulation the associated noise figure $F_{Loop}^{(n)}$ is

$$\begin{aligned} F_{Loop}^{(N)} &= F_{Loop} + \frac{F_{Loop} - 1}{G_{Loop}} + \frac{F_{Loop} - 1}{G_{Loop}^2} + \cdots + \frac{F_{Loop} - 1}{G_{Loop}^{N-1}} \\ &= F_{Loop} + \frac{F_{Loop} - 1}{G_{Loop}^{N-1}} \frac{1 - G_{Loop}^{N-1}}{1 - G_{Loop}} \end{aligned} \tag{4}$$

where G_{Loop} is the loop gain,

$$G_{Loop} = \frac{G_{SOA}}{L_I L_t L_{ex}} \tag{5}$$

where $L_t = 1 - L_c$ is the coupler thru loss. Since the link output is to be the periodic extension of the input, the SOA gain is adjusted so that $G_{Loop} = 1$ so that Equation (4) becomes

$$F_{Loop}^{(N)} = N\left(F_{Loop} - 1\right) + 1 \tag{6}$$

Equation (6) shows that although after many loop circulations the signal will be largely corrupted by noise, it is still reasonable to expect that for values of integer N sufficiently small, a signal with a reasonable SNR can still exist in the loop. It will be seen later that values significantly greater than $N = 100$ are quite reasonable.

Note also that some additional degradation in SNR occurs due the initial and final coupling into and out of the loop. This overall (optical) noise figure $F^{(N)}$ is given by (again for the case of unity loop gain)

$$F^{(N)} = \begin{cases} L_t, & N = 0 \\ L_c L_I \dfrac{G_{SOA}F_{SOA} - 1 + L_c L_{ex}}{G_{SOA}}, & N = 1 \\ L_c \dfrac{G_{Loop}^{N+1} G_{SOA} F_N + G_{SOA} L_I F_{SOA} + L_I L_c L_{ex} - L_I - G_{SOA}}{G_{SOA} G_{Loop}}, & N > 1 \end{cases} \tag{7}$$

The SNR characteristics for direct-detection analog fiber optic link with external or direct modulation are well known [13]. The present discussion then serves only to indicate the manner by which the recirculating delay loop impacts the overall noise of the system. Three significant noise sources are present; input noise, detector noise (primarily shot, thermal, and dark current noise), and laser noise. The average noise power introduced in the detection process is designated, $P_{Detector\ Noise}$ and is not effected by the presence of the recirculating loop. The average laser noise power, designated as $P_{Laser\ Noise}$, is primarily a result of the relative intensity noise (n_{RIN}). Finally, the noise present at the modulator input, generally thermal noise, contributes a term $P_{Input\ Noise}$. The total electrical average noise power at the detector output can be expresses as

$$P_{Total\ Noise} = P_{Detector\ Noise} + G_{RF} P_{RF\ Input\ Noise} + F_o(0)\, n_{RIN} \tag{8}$$

where $F_o(0)$ is the link noise figure in the absence of the recirculating loop and is given by

$$F_o = \frac{1 - \eta_{ex} + \eta_{ex} L_t}{\eta_{ex} \eta_{mod}} \tag{9}$$

and where the link RF gain is

$$G_{RF} = \frac{p_{out}}{p_{in}} = \left(\frac{\pi \rho \eta_{ex}^{-1} \cdot \eta_{mod}^{-1} \cdot G_N P_o |Z_{mod}|}{V_\pi} \right)^2 \frac{R_L}{R_{mod}} \tag{10}$$

In equation (10) η is the link gain/loss, P_o is the laser power, ρ is the detector responsivity, V_π represents the modulator extinction voltage, R_L is the load impedance, and Z_{mod} is the modulator input impedance with R_{mod} =Re{Z_{mod}}

The major controllable factor influencing the total is due to the laser RIN, which can be minimized by using a solid-state laser. The system SNR can be further reduced using coherent detection but at the expense of a more complicated system.

From equation (2), the noise figure $F(N)$ representing the degradation in SNR after N loop-circulations can be expressed,

$$F_{RF}(N) = \left.\frac{SNR_{without\ loop}}{SNR_{with\ loop}}\right|_{Same\ Link\ Gain} = \frac{n_d + G_{RF} n_{RF\ input} + F_o(N) n_{RIN}}{n_d + G_{RF} n_{RF\ input} + F_o(0) n_{RIN}} \tag{11}$$

where the noise figure with the recirculating loop present is given by

$$F_o(N) = \frac{1 - \eta_{ex} + \eta_{ex} L_t \left(L_t + F^{(N)} - 1 \right)}{\eta_{ex} \eta_{mod}} \tag{12}$$

Equation (11) assumes $G_{Loop} = 1$ and that the coupler ratio L_c is chosen to maintain the same link gain for no passes as for *N*-passes.

Since the *SNR* and link resolution *B* are related by equation (1), equation (11) allows the computation of the effective number of bits of the ADC as follows. Let B_o represent the link resolution without the recirculating loop and let B_{eff} be the resolution with the recirculating loop present. Then,

$$SNR_{with\ loop} = \frac{SNR_{without\ loop}}{F_{RF}(N)} = \frac{3}{2} \frac{2^{2B_o}}{F_{RF}(N)} = \frac{3}{2} 2^{2B_{eff}} \tag{13}$$

Solving for B_{eff} gives

$$B_{eff} = B_o - \frac{1}{2}\log_2 F_{RF}(N) \tag{14}$$

We see that the degradation in the SNR increases logarithmically with noise figure $F(N)$. With regard to the present system architecture the ADC performance can be captured effectively in terms of a reduction in the ENOB, $B_r = B_o - B_{eff}$ or

$$B_r = \frac{1}{2}\log_2 F_{RF}(N) \tag{15}$$

To estimate expected performance, Table (1) provides typical operational values for the components that constitute the recirculating delay loop. From these, estimates for the corresponding noise figure as a function of the number of loop circulations can be obtained from Equation (11) and, more significantly, the reduction in the ENOB can be computed from Equation (15).

Table 1: Typical Loop Component Parameters

Quantity	Value	Units
3-dB Coupler Insertion Loss	4.0	*dB*
Total Excess Loop Loss	3.0	*dB*
SOA Noise Figure	4.0	*dB*

For these estimates, the SOA gain was chose to exactly cancel the loop loss (~ 4.5 dB). This gives from Equation (3) a loop noise figure of just over 7.7 dB. Figure (3) shows this effect in terms of the reduction in the ENOB. It is seen that even after several hundred-loop circulations the ENOB has been reduced by roughly four bits. This means that a link capable of resolving the desired number of bits plus the bit reduction is required. To place this in perspective, note that a 10 - bit ADC requires a Spur-Free Dynamic Range (SFDR) of roughly 60.4 dB. The present approach thus requires the ability to resolve 14-bits, or a SFDR of roughly 83.7 dB in a 5 GHz bandwidth for a 10 Gsps ADC. Expressed in terms if of a 1 Hz bandwidth, a

SFDR of 148.3 dB is required. State-of-the-art broadband (18 GHz) analog fiber optic links have a SFDR approaching 130 dB, hence, at the reduced bandwidth the link requirement, though challenging, is within reach. Commercial ADC systems have been reported with an ENOB of (roughly) 10-bits with sampling frequencies in excess of 100 MHz [3]. This suggests that the photonically assisted system presented here with N = 100 would potentially yield a 10 Giga-sample per second ADC with the required ten bits of resolution. However, other factors must also be considered which also limit the ENOB. As mentioned previously, the aperture uncertainty requirements are those of the high-speed ADC. The effective number of bits as a function of timing jitter is given by

$$\tau_a = \frac{1}{\sqrt{3}\, f_{sample}} 2^{-B} \tag{16}$$

from which we find that a 10-bit, 10 Gsps ADC requires an aperture uncertainty of roughly 65 fsec, another challenging requirement that can be met with a mode-locked (pulsed) laser clocking system, since solid-state clocks generally can provide uncertainties on the order of 1 ps [14].

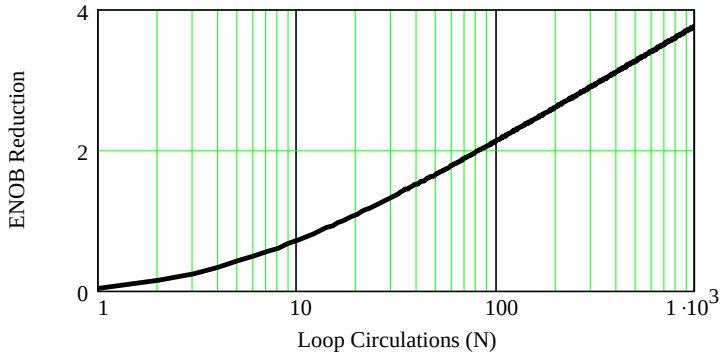

Figure 3: Reduction in effective number of bits as a function of the number of loop-circulations.

3. EXPERIMENTAL RESULTS

The system of Figure (1) was constructed on an optical bench. A 1550 nm, 0.5 mw diode laser was used as the optical source. The link was modulated using an 18 GHz - $LiNbO_3$ Mach-Zehnder modulator. To generate the time limited RF input signal, a computer was used to toggle

on then off a synthesized signal generator (operating for the purpose of this demonstration at a frequency of 900 MHz) to produce a 1 – microsecond RF burst. The RF signal drives the EO modulator near the maximum power level of 20 dBm. The RF modulated optical signal was injected into the recirculating delay loop via a 3 dB coupler. A loop time delay of roughly 5 - microseconds was achieved using 1 Km of single mode fiber with fine time delay adjustment ($\pm$ 3 nanoseconds) obtained from a variable delay line. Note that the loop time delay is designed so that the RF signal is always shorter in duration than the loop delay and so a coherent addition of the RF components would never occur from period to period. Upon exiting the loop via the 3-dB coupler, the signal is directed to a 99:1 splitter with the 1% output used to monitor the steady-state optical signal on an (optical) spectrum analyzer. The 99% port is connected to a 2 GHz PIN photodetector, and the resulting periodic signal is viewed on a high-speed oscilloscope. Note that the experimental did not include an optical switch as a means to purge the signal in the loop. For our purposes, this switching was accomplished by using the SOA driver to turn off the SOA between data measurements. Also note that since the system was constructed with (connectorized) bulk optical components, this resulted in reduced SNR performance. The actual operational layout of the system along with its measurement apparatus is shown in Figure (4) while the schematic representation of the system is shown in Figure (5).

Time domain performance data is shown in Figures (6) and (7). Specifically Figure (6) a rather arbitrarily shaped input signal containing both low and high frequency components was generated by toggling an RF source on, then off, using a GBIP controller. It is seen that the shape is preserved as the signal circulates. The low frequency roll-off was caused by the limited low-end frequency response of the electronic amplifiers used. Figure (7) shows the output for an input signal consisting of a sinusoidal tone burst. Here it is seen that the signal is corrupted by laser noise bursts. A means to eliminate this noise is suggested later in the next section of this report.

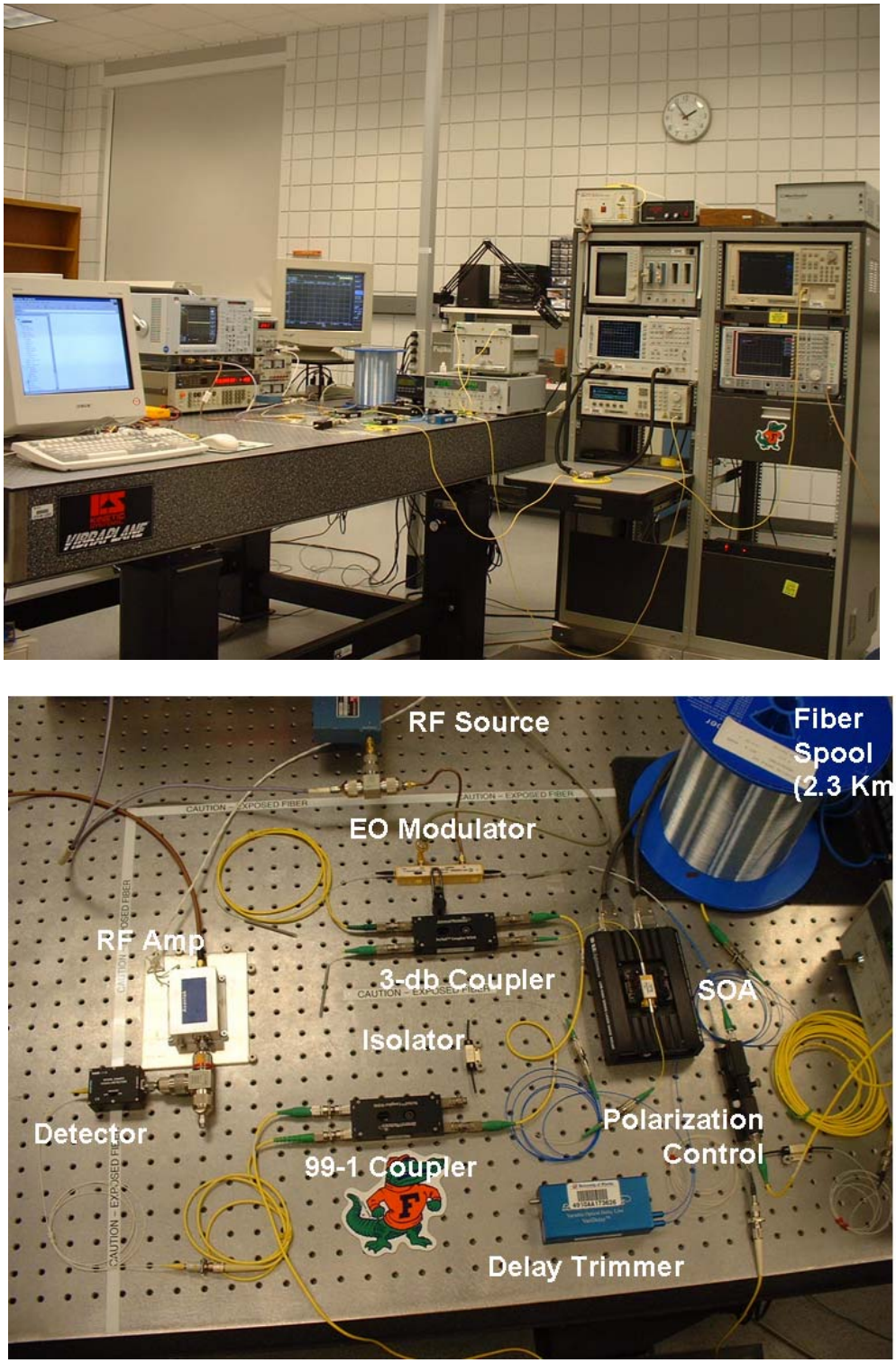

Figure 4: Experimental Setup – Physical layout

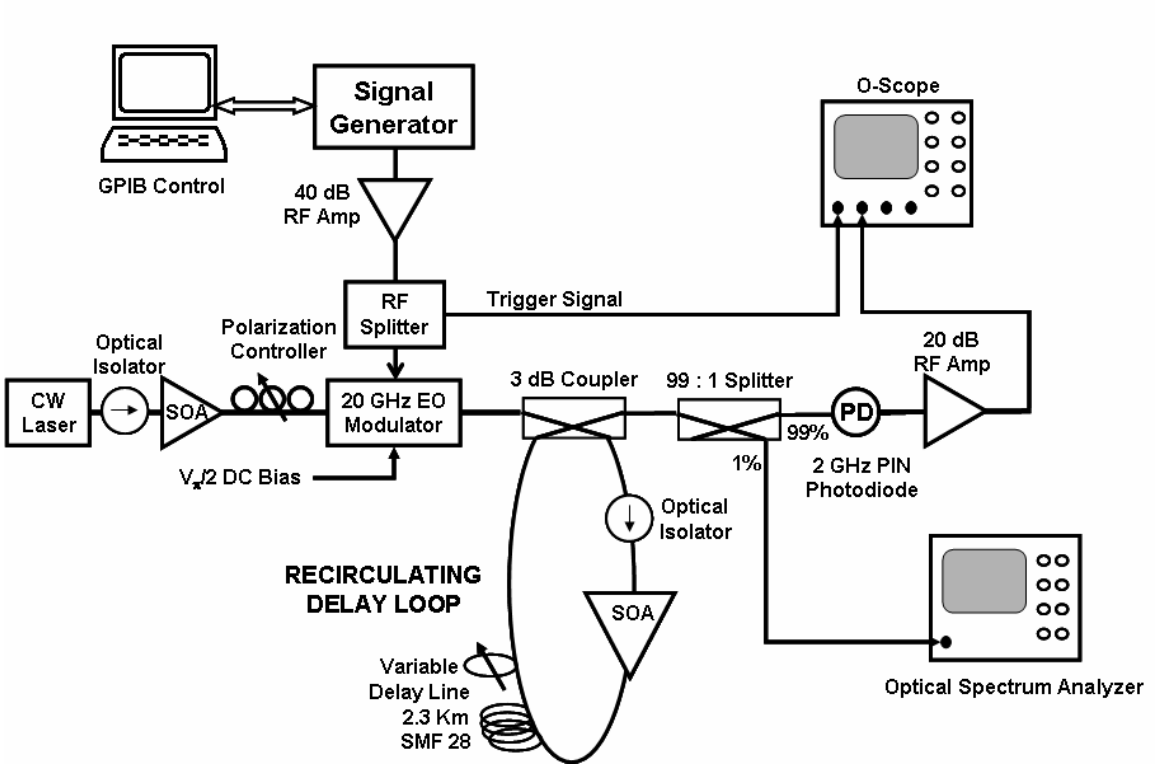

Figure 5: Experimental Setup – Schematic representation and measurement setup.

Table 2: Experimental Parameters

Quantity	Value	Units
Wavelength	1550	nm
Laser Power	5.0	mw
Detector Responsivity	0.95	Amps/Watt
Detector Bandwidth	2.0	GHz
Laser RIN	-145	dB/Hz

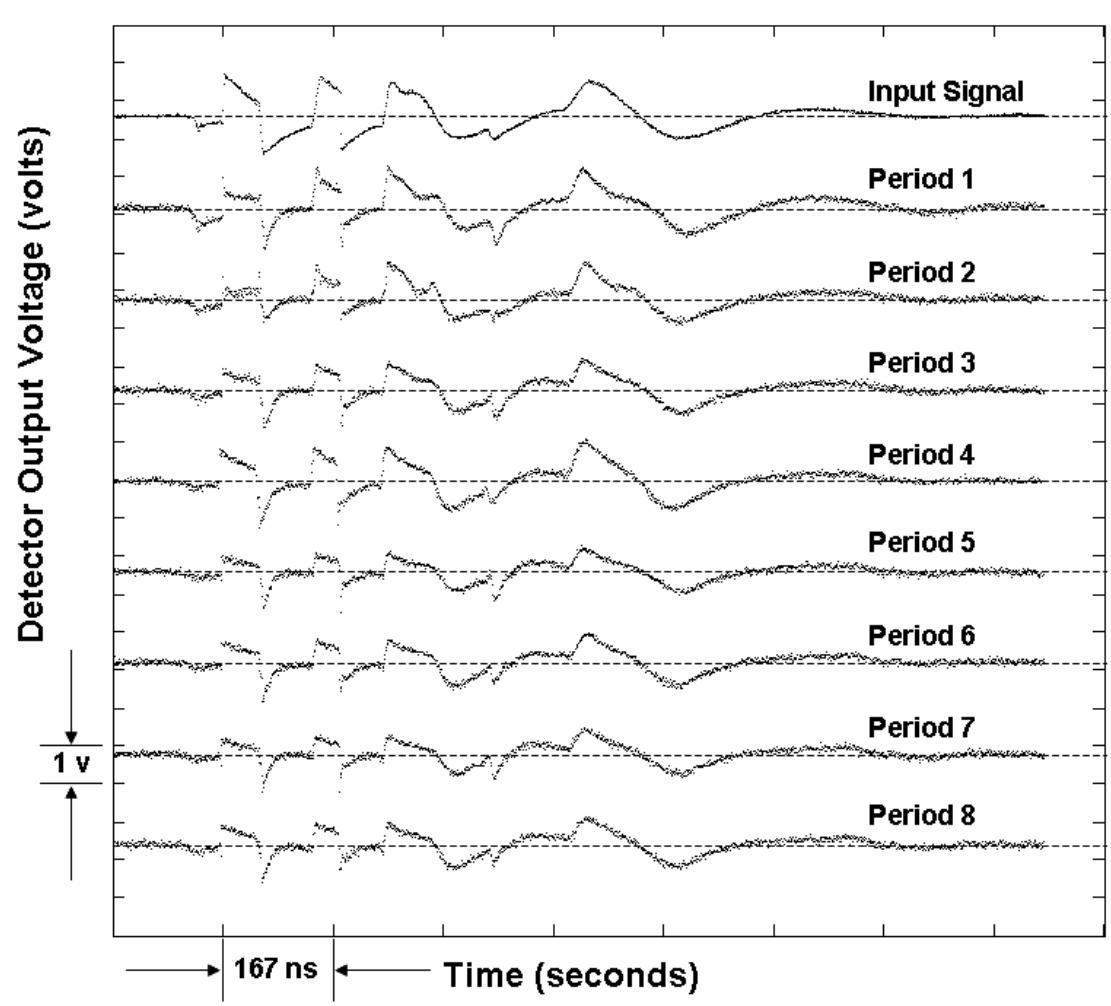

Figure 6: Measured output voltage for first eight period with for an arbitrarily shaped input pulse.

Figure 7: (a) Measured output for first seven periods, and (b) with a 500 µ sec. delay.

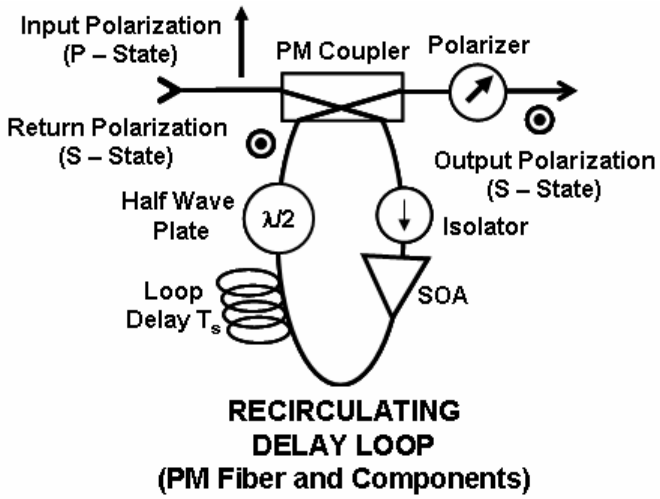

Figure 8: Polarization management to suppress laser noise.

3.1 Recommendations to eliminate polarization noise.

The system was constructed using components that were all polarization insensitive. This resulted in most instances in a return optical signal that was like-polarized with the input optical signal. Since the gain of the recirculating loop is adjusted to unity, there was a tendency for the system to lase. Since the loop contained no wavelength selective components, lasing could not occur in the strict sense. However, naturally occurring peaks in the optical amplifiers spectral response resulted in random temporal "bursts" of optical signal appearing as added noise in the detected RF signal. To eliminate this from occurring, the polarization management shown in Figure 5 can be used. The light exiting the modulator has a known State of Polarization (SOP). A Polarization Maintaining (PM) coupler would launch a portion of the light into the recirculating loop as before. For the experimental results given here, PM components were not employed in the loop resulting in the significant polarization drift observed in the measured data. Using PM fiber in the loop along with all PM components would maintain the SOP as the light exits the excess fiber that then re-enters the PM coupler. If, before this light re-enters the coupler, a half-wave plate is used to rotate the SOP by 90-degrees, then the light that recombines with the light from the input laser will be orthogonally polarized with respect to each other thus introducing a high polarization loss factor thus suppressing any lasing in the loop. A polarizer is then used just before the detector to eliminate the unwanted light that would otherwise contribute to shot noise in the detector. These modifications are currently being made to the ADC system and will be reported on at a later time.

4. CONCLUSIONS

This report has presented a design for a simple yet effective way of implementing an ADC with the potential to achieve both high-speed and high resolution. Preliminary data, obtained form a tabletop implementation, demonstrates, at least in-principle, the validity of the proposed ideas. A distinct advantage is that the ADC system can be realized by the appropriate modification of an existing fiber optic link. Furthermore, it was shown that the inclusion of the recirculating delay loop used to modify the link results in only a minimal reduction in the effective number of bits. Consequently the performance of the present ADC system improves as both fiber optic link technology and electronic ADC technology improves. Since these are the

subject of great interest in the microwave photonics community, such improvements can be expected. This report further quantified and provided accurate analytical estimates for critical parameters such as the ENOB, the overall noise figure, and the sampling rate.

The most severe restrictions on the ENOB arise from the required SFDR and aperture uncertainty. These restrictions are especially critical for broadband links that are generally thermal noise limited. Quantum limited detection is possible by using coherent detection but at the expense of a somewhat more complicated system and now with the concerns of added phase noise. The dynamic range of fiber optic links can be extended, in some cases significantly, by a variety of techniques. These include linearizing the output of the EO modulator by pre-distorting the input signal or by linearizing the modulator itself by utilizing multiple modulators to subtract out some of the nonlinear effects of a single Mach-Zehnder device. Though such approaches have proven effective, these techniques typically have sub-octave bandwidths and result in a more complicated system [16].

Since the noise figure of the recirculating delay loop represents a major source of SNR degradation, especially for a large number of circulations, it is important to reduce the laser (RIN) noise as must as possible. The RIN noise may be reduced to almost immeasurable levels by using a solid state laser source instead of the more common semiconductor or fiber laser.

Another inherent limitation with this approach is time required for digitization of a time packet T seconds long. The N – loop circulation needed to obtain all the samples, a processing time of approximately NT seconds is required. Because of the simplicity of the ADC structure, this drawback can be mitigated to some extent by using a time-multiplexed multiple ADC approach as is sometimes employed in the design of high-speed oscilloscopes. Other ways of addressing this issue involve the use of multi-wavelength systems and are currently under investigation. On the other hand, many high-speed applications such as radar only operate on a finite time portion of a signal so that the present system may be adequate.

A final concern, in fact one that exists for *any* high-speed ADC, is the timing accuracy of the signal samples. Though the present approach allows for the implementation of a “fast” ADC from a slower electronic ADC, the timing accuracy (jitter) for the slow ADC used in the implementation would likely not be sufficient for the high-speed operation. Adequate clock stability would require a separate timing unit for the ADC system. Since a suitable stable clock is an essential component for any ADC system, timing circuits employing stable mode-locked-

lasers are being studied by several investigators [14]. Timing stability concerns may also require that portions of the system, especially the recirculating loop, be placed in a temperature-controlled environment as is often done with high-speed test equipment. All of the above concerns discussed are currently under investigation and will be reported on at a later time.

REFERENCES

1. H.F. Taylor, "An Optical Analog-to-Digital Converter," *IEEE Journal of Quantum Electronics*, Vol. QE-15, pp. 210-216, 1979.

2. R.G Walker, I. Benian, and A.C, Carter, "Novel GaAs/AlGaAs Guided Wave Analogue/Digital Converter," *Electronics Letters*, Vol. 25, pp. 1443-1444, Oct. 1989.

3. R.H. Walden, "Analog-to-digital converter survey and analysis," *IEEE Journal of Selected Areas in Communications*, pp. 539-550, 1999.

4. T.R. Clark, Jr., and M.L. Dennis, "Toward a 100-Gsample/s Photonic A-D Converter" *IEEE Photonics Technology Letters*, Vol. 13, No. 3, March 2001, pp. 236-238.

5. M.J. Hayduk, R.J. Bussjager, and M.A. Getbehead, "Photonic Analog to Digital Conversion Techniques Using Semiconductor Saturable Absorbers," *Proc. SPIE*, pp. 1-7, April, 2000.

6. M. Johansson, B. Lofving, S. Hard, L. Thylen, M. Mokhtare, U. Westergren, and C. Pala, "Study of an Ultrafast Analog-to-Digital Conversion Scheme Based on Diffractive Optics," *Applied Optics*, **29**, no. 17, pp. 2881-2887, 10 June 2000.

7. E.N. Toughlian and H. Zmuda, "A Photonic Wide-Band Analog to Digital Converter," International Topical Meeting on Microwave Photonics- MWP 2000, 11-13 September, Oxford, UK, pp. 248-250.

8. M.Y. Frankel, Jin U. Kang, and R.D. Esman, "High-performance photonic analogue-digital converter", *Electronic Letters*, Vol. 33, pp 2096-2097, Dec. 1997.

9. Jin U. Kang, M.Y. Frankel, and R.D. Esman, "Highly parallel pulsed optoelectronic analog-digital converter", *IEEE Photonics Technology Letters*, Vol. 10, pp. 1626-1628, Nov. 1998.

10. J.A. Bell. M.C. Hamilton, D.A. Leep, "A/D Conversion of Microwave Signals Using a Hybrid Optical/Electronic Technique," *Proc. SPIE*, **1476**, pp 326-329, 1991.

11. P.E. Pace and D. Dtyer, "High-Resolution Encoding Process for an Integrated Optical Analog-to-Digital Converter," *Optical Engineering*, **33**, no. 8, pp. 2638-2645, August 1994.

12. B. Jalali, F. Coppinger, A.S. Bushan, "Time-Stretch Preprocessing Overcomes ADC Limitations," *Microwaves & RF*, pp. 57-66, March 1999.

13. E. Ackermann, "RF Fiber-Optic Links," in Photonic Aspects of Modern Radar, H. Zmuda and E.N. Toughlian, editors, Boston: Artech House, 1994, pp.323-350.

14. W. Ng, R. Stephens, D. Persechini, and K.V. Reddy, "Ultra Low Jitter Mode-Locking of Er-Fiber Laser at 10 GHz and its Application to Photonic Analog-to-Digital Conversion," International Topical Meeting on Microwave Photonics- MWP 2000, 11-13 September, Oxford, UK, pp. 251-254.

15. E.I Ackermann, "Broad-Band Linearization of a Mach-Zehnder Electrooptic Modulator," *IEEE Transaction on Microwave Theory and Techniques*, Vol. 47, No. 12, pp. 2271-2279, Dec. 1999.

16. U.V. Cummings and W. B. Bridges, "Bandwidth of Linearized Electrooptic Modulators," *IEEE Journal of Lightwave Technology*, Vol. 16, No. 4, pp. 1482-1490, Aug. 1998.